Protein Science (1997), 6:383–390. Cambridge University Press. Printed in the USA.

Complete ^{1}H, ^{13}C, and ^{15}N NMR resonance assignments and secondary structure of human glutaredoxin in the fully reduced form

CHAOHONG SUN,[1] ARNE HOLMGREN,[2] AND JOHN H. BUSHWELLER[1]

[1] Department of Chemistry, Dartmouth College, Hanover, New Hampshire 03755
[2] Medical Nobel Institute for Biochemistry, Department of Medical Biochemistry and Biophysics, Karolinska Institute, S-171 77 Stockholm, Sweden

(RECEIVED July 31, 1996; ACCEPTED November 4, 1996)

Abstract

Human glutaredoxin is a member of the glutaredoxin family, which is characterized by a glutathione binding site and a redox-active dithiol/disulfide in the active site. Unlike *Escherichia coli* glutaredoxin-1, this protein has additional cysteine residues that have been suggested to play a regulatory role in its activity. Human glutaredoxin (106 amino acid residues, M_r = 12,000) has been purified from a pET expression vector with both uniform ^{15}N labeling and $^{13}C/^{15}N$ double labeling. The combination of three-dimensional ^{15}N-edited TOCSY, ^{15}N-edited NOESY, HNCA, HN(CO)CA, and gradient sensitivity-enhanced HNCACB and HNCO spectra were used to obtain sequential assignments for residues 2–106 of the protein. The gradient-enhanced version of the HCCH-TOCSY pulse sequence and HCCH-COSY were used to obtain side chain ^{1}H and ^{13}C assignments. The secondary structural elements in the reduced protein were identified based on NOE information, amide proton exchange data, and chemical shift index data. Human glutaredoxin contains five helices extending approximately from residues 4–10, 24–36, 53–64, 83–92, and 94–104. The secondary structure also shows four β-strands comprised of residues 15–19, 43–48, 71–75, 78–80, which form a β-sheet almost identical to that found in *E. coli* glutaredoxin-1. Complete ^{1}H, ^{13}C, and ^{15}N assignments and the secondary structure of fully reduced human glutaredoxin are presented. Comparison to the structures of other glutaredoxins is presented and differences in the secondary structure elements are discussed.

Keywords: glutaredoxin; nuclear magnetic resonance; secondary structure; sequence-specific assignments

Glutaredoxins are small proteins (M_r = 12,000) involved in electron transfer reactions via the reversible oxidation of two SH groups to a disulfide bond in the active site. The Grx active site sequence Cys-Pro-Tyr-Cys is highly conserved among a variety of different organisms, including *Escherichia coli*, vaccinia virus, yeast, plants, and mammalian cells (Höög et al., 1983; Klintrot et al., 1984; Gan & Wells, 1987a; Gan et al., 1990; Hopper et al., 1989; Johnson et al., 1991; Ahn & Moss, 1992; Minakuchi et al., 1994; Padilla et al., 1995). Grx is essential for the glutathione-dependent synthesis of deoxyribonucleotides by ribonucleotide reductase (Holmgren, 1976, 1979a; Luthman et al., 1979; Luthman & Holmgren, 1982). Glutaredoxin has inherent glutathione-disulfide oxidoreductase activity in a coupled system with GSH, NADPH, and glutathione reductase (Holmgren, 1979a, 1989), catalyzing the reduction of low molecular weight disulfides as well as proteins. A binding site for glutathione has been identified on *E. coli* glutaredoxin-1 (Bushweller et al., 1994), providing a rationale for the preference of glutaredoxin for glutathione-containing disulfides. Grx has been proposed to exert a general thiol redox control of protein activity by acting both as an effective protein disulfide reductase (Holmgren, 1985; Ziegler, 1985) and as a specific GSH-mixed disulfide reductase (Gravina & Mieyal, 1993). In addition, glutaredoxin exhibits dehydroascorbate reductase activity, suggesting a function to defend cells against oxidative stress (Wells et al., 1990).

The glutaredoxin family of proteins is distinguished from the thioredoxin family of proteins on the basis of their differential reactivity. Glutaredoxins are reduced by GSH (which is, in turn, reduced by glutathione reductase) but not by thioredoxin reductase, whereas thioredoxins are reduced by the corresponding thioredoxin reductases but not by GSH; thus, these two families of proteins represent independent sources of reducing equivalents. In addition, glutaredoxin catalyzes GSH-disulfide oxido-reduction reactions, unlike thioredoxin, which acts as a quite general protein

Reprint requests to: John H. Bushweller, Department of Chemistry, Dartmouth College, Hanover, New Hampshire, 03755; e-mail: john.bushweller@dartmouth.edu.

Abbreviations: DTT, dithiothreitol; Grx, glutaredoxin; Grx1, *E. coli* glutaredoxin-1; Grx3, *E. coli* glutaredoxin-3; GSH, Glutathione; HED, β-hydroxyethyl disulfide; IPTG, isopropyl β-D-thiogalactopyranoside.

disulfide reductase (Holmgren, 1979b, 1985). Thioredoxin and glutaredoxin belong to a large class of proteins catalyzing redox reactions in the cell. For several members of this class, three-dimensional structures have been reported; for example, for the oxidized form of *E. coli* thioredoxin by X-ray crystallography (Katti et al., 1990), for the reduced and oxidized forms of *E. coli* thioredoxin by NMR (Dyson et al., 1990; Jeng et al., 1994), for the reduced and oxidized forms of human thioredoxin by NMR (Forman-Kay et al., 1991; Qin et al., 1994), for the oxidized and reduced forms of T4 glutaredoxin by X-ray crystallography (Eklund et al., 1992; Ingelman et al., 1995), for pig liver thioltransferase by X-ray crystallography (Katti et al., 1995), and for oxidized, reduced, and glutathione mixed-disulfide forms of *E. coli* glutaredoxin-1 by NMR (Sodano et al., 1991; Xia et al., 1992; Bushweller et al., 1994).

All the mammalian glutaredoxins studied thus far have two cysteine residues in addition to those observed in the active site. These additional cysteine residues have been proposed to play a regulatory role, because their oxidation leads to inactivation of enzyme activity in the case of calf thymus glutaredoxin (Klintrot et al., 1984). These cysteines are part of a group of amino acids conserved among the transforming growth factor-β (TGF-β) family and mammalian glutaredoxins (Guigó & Smith, 1991), leading credence to the notion of this motif as a potential site for redox regulation.

As seen in Figure 1, glutaredoxins show a high degree of homology in the vicinity of the active site, as expected because this is the location of the glutathione binding site (Bushweller et al., 1994). However, outside these regions, the homology between mammalian glutaredoxins and *E. coli* glutaredoxin breaks down. Human glutaredoxin is longer than its *E. coli* counterpart (106 versus 85 amino acids) and is a basic protein unlike *E. coli*, thus it is of significant interest to determine the structure of the human glutaredoxin. In addition, the presence of this potential site of redox regulation provides a unique opportunity to examine the structural implications of this increasingly common phenomenon in this system. The recent cloning and high-level expression of human Grx in *E. coli* (Padilla et al., 1996) have provided us with ample quantities of protein to pursue structural studies of this protein. Herein we report the heteronuclear assignments and secondary structure of human glutaredoxin in its fully reduced form.

Results

2D HSQC

Figure 2 shows a two-dimensional ^{15}N-^{1}H HSQC spectrum of human glutaredoxin in the fully reduced form. Despite the moderately low amide proton dispersion, there are only four cases of completely degenerate signals, F18/D47, Q58/V87, K77/Q90, and E94/I80. Additionally, the resonances of all five of the expected arginine ϵ-amino groups are resolved. For the side-chain resonances of Gln and Asn, a total of 30 peaks are resolved with several cases of near degeneracy.

Backbone assignment strategy

Assignments of human glutaredoxin began from the HNCA and HN(CO)CA data. These experiments correlate the intraresidue and interresidue C_α in the case of HNCA and the interresidue C_α only in the case of HN(CO)CA. It was clear that these two spectra alone would not be adequate for this protein due to degeneracies in the C_α resonances.

The recent introduction of experiments such as HNCACB (Wittekind & Mueller, 1993) and CBCA(CO)NH (Grzesiek & Bax, 1992) has provided an independent route for assignments through the C_β resonances, wherein the ambiguity present in data from HNCA/HN(CO)CA arising from degeneracies in C_α frequencies is almost always overcome. High-quality HNCACB data were collected for human Grx using the gradient sensitivity-enhanced pulse sequence of Muhandiram and Kay (1994).

The HNCACB spectrum, which correlates both intraresidue and interresidue C_α and C_β resonances with the NH resonance, was then employed to complete the backbone assignment process. By searching [ω_2(^{13}C), ω_3(NH)]-strips at the ^{15}N frequencies obtained from the ^{15}N-^{1}H HSQC spectrum in the HNCACB spectrum in a semi-automated fashion using the program XEASY (Bartels et al., 1995), neighboring residues were identified readily on the basis of the common C_α, C_β shifts observed for neighboring residues. Data from the HN(CO)CA spectrum were used to confirm the sequential assignments. The unique chemical shifts observed for Gly, Ser, Thr, and Ala residues provided checkpoints in the assignment process.

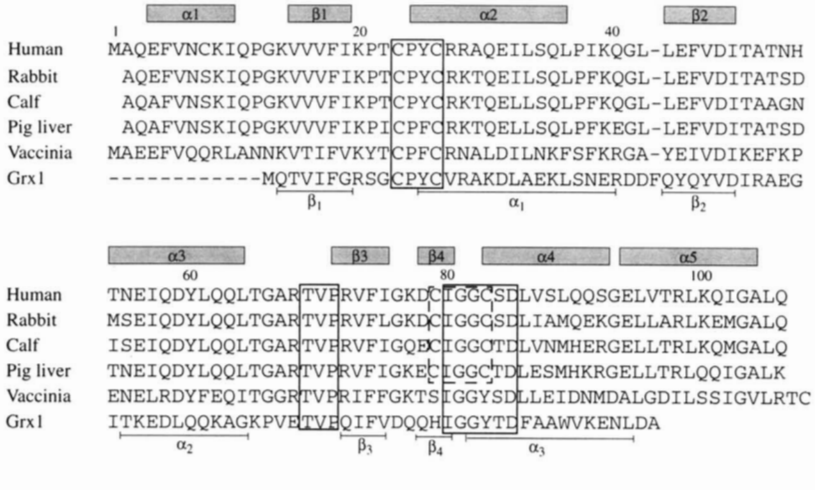

Fig. 1. Comparison of the amino acid sequence of human glutaredoxin with other known glutaredoxins. Numbering given is that for human glutaredoxin. Residues bordering the glutathione binding site in *E. coli* glutaredoxin-1 are outlined in solid boxes. The additional two cysteine residues found in the mammalian glutaredoxins are outlined in a dashed box (Höög et al., 1983; Klintrot et al., 1984; Gan & Wells, 1987a; Hopper et al., 1989; Papayannopoulos et al., 1989; Johnson et al., 1991; Padilla et al., 1995). The secondary structure for glutaredoxin-1 is shown with line segments under the *E. coli* Grx1 sequence. The secondary structure of human Grx as determined by NMR spectroscopy is indicated with boxes above the human Grx sequence.

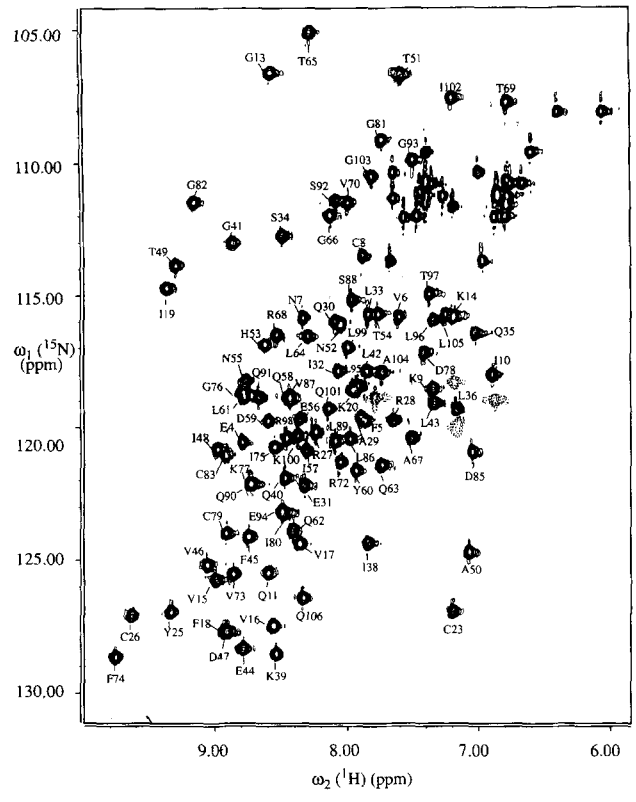

Fig. 2. Contour plot of the region [ω_1 (^{15}N) = 104–131 ppm; ω_2 (^{1}H) = 5.9–9.4 ppm] in the ^{15}N-^{1}H HSQC spectrum of reduced human glutaredoxin. Assignments for the backbone NH peaks are indicated.

In order to provide an additional unique pathway for resonance assignments, as well as to obtain assignments for the H_α resonances necessary for side-chain assignment, we also recorded an HN(CA)HA spectrum (Clubb et al., 1992). This experiment correlates the intraresidue and interresidue H_α resonances with the NH and thus provides a unique check on the assignments made above. All the above assignments were confirmed in this manner and H_α assignments were obtained. Intraresidue and interresidue H_α resonances were distinguished on the basis of ^{15}N-edited three-dimensional TOCSY data collected earlier on an ^{15}N-labeled sample.

Side-chain resonance assignments

Based on the unique H_α and C_α resonance assignments described above, the H_α/C_α region of the [^{13}C-^{1}H] CT-HSQC spectrum was assigned. These H_α/C_α peaks were then used as the anchor points for the assignments of the aliphatic side chains. Assignments for the aliphatic side-chain resonances were obtained from HCCH-TOCSY (Kay et al., 1993) and HCCH-COSY (Ikura et al., 1991) spectra with reference to the C_β data obtained from the HNCACB spectrum. HCCH-TOCSY data were recorded with mixing times of 8 and 21 ms to provide single and multi-step side-chain correlations, respectively. The HCCH-COSY data were employed to obtain definitive identification of neighboring carbons and hydrogens in the aliphatic side chains.

The limited bandwidth of the DIPSI-3 mixing sequence used in the HCCH-TOCSY experiment did not allow correlations to be obtained to the aromatic rings. In order to complete these assignments, two- and three-dimensional versions of the $(H_\beta)C_\beta(C_\gamma C_\delta)H_\delta$ and $(H_\beta)C_\beta(C_\gamma C_\delta C_\epsilon)H_\epsilon$ experiments of Kay and coworkers (Yamazaki et al., 1993) were recorded. These experiments provide direct correlations between the C_β resonances (as well as H_β in the case of the three-dimensional version) and the protons of the aromatic rings. HCCH-TOCSY and DQF-COSY data were employed to check the assignments and extend them to H_ζ in the case of the phenylalanines. Aromatic ring assignments are complete with the exception of Phe 45, for which the H_ζ could not be identified.

The side-chain amide resonances of Gln and Asn were assigned via a combination of HNCACB and ^{15}N-edited NOESY data. As described by Wittekind and Mueller (1993), the HNCACB experiment can be modified slightly to obtain correlations for the side-chain amides of Gln and Asn. These data were adequate for the assignment of all the Asn residues; however, degeneracies were observed in the C_β and C_γ chemical shifts of six of the Gln residues. In these cases, NOEs between the side-chain amide protons and the aliphatic H_γ and H_β protons observed in a 120-ms three-dimensional ^{15}N-edited NOESY spectrum were used to resolve these ambiguities. The HNCACB and NOESY data also provided assignments for the HNϵ of the arginine residues.

Chemical shifts of all assigned ^{1}H, ^{13}C, and ^{15}N nuclei are listed in the table in the supplementary material provided in the Electronic Appendix.

Secondary structure determination

Regular secondary structure elements in proteins give rise to characteristic NOEs (Wüthrich, 1986) that can be used to identify the boundaries of these elements. Particularly in α-helices, a dense array of sequential and medium-range NOEs are observed that provide definitive identification of these elements. These include NH(i)-NH(i + 1), NH(i)-NH(i + 2), $H_\alpha(i)$-NH(i + 3), $H_\alpha(i)$-NH(i + 4), and $H_\alpha(i)$-$H_\beta(i + 3)$ NOEs. In the case of β-strands, strong sequential $H_\alpha(i)$-NH(i + 1) NOEs are observed, as well as H_α-NH and H_α-H_α NOEs across the strands of a β-sheet. These interstrand NOEs can be used for determination of the topology of the β-sheet as well as to define the ends of β-strands.

The hydrogen bonded amide protons of helices and β-sheets display slowed exchange upon dissolution in D_2O buffer; thus this provides an additional means of identifying those residues involved in regular secondary structures. In addition, the chemical shifts of the backbone atoms H_α, C_α, C_β, and C′ have been shown to have a strong correlation with the secondary structure of the residue involved (Spera & Bax, 1991; Wishart & Sykes, 1994). Recently, Wishart and Sykes have developed a chemical shift index (CSI) based on the chemical shifts of all four nuclei that predicts the secondary structure with relatively high accuracy. Figure 3 summarizes the sequential and medium-range NOEs observed, the amide proton exchange data, and the CSI data for human glutaredoxin.

Discussion

As seen in Figure 3, analysis of the secondary structure of human glutaredoxin shows it to be an α/β protein, as are all the other glutaredoxins for which structural information is available. N-terminal sequencing showed that the N-terminal methionine is proteolytically cleaved off, as demonstrated previously (Padilla et al., 1996); thus the assignments begin from the Ala in position 2 of the cDNA sequence. The protein contains a total of five

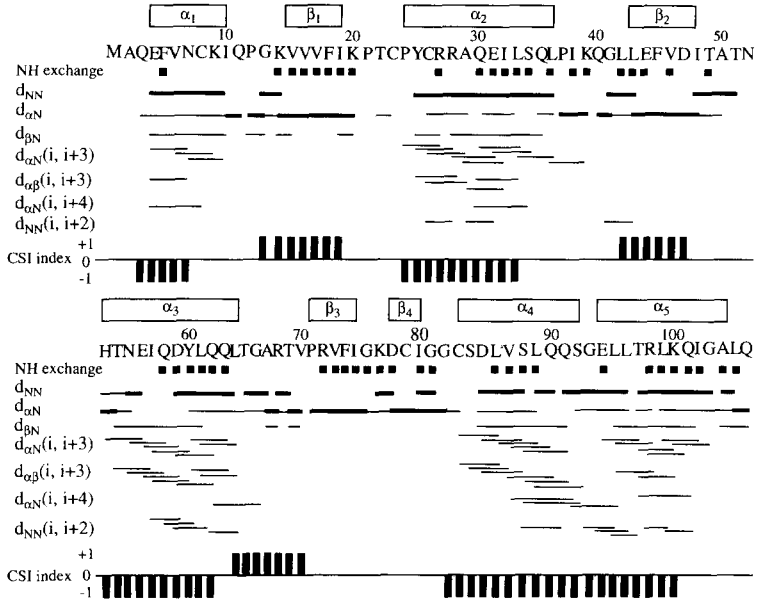

Fig. 3. Primary sequence of human glutaredoxin with a summary of observed short- and medium-range NOEs, NH exchange data, and the CSI data (Wishart & Sykes, 1994). Squares below the sequence indicate residues with amide protons still visible in a two-dimensional [^{15}N, ^{1}H] HSQC spectrum after 2 h of solvent exchange in D_2O buffer at pH 6.0, 10 °C. Regular secondary structures are shown above the sequence. The consensus CSI data obtained from $^{1}H_{\alpha}$, $^{13}C_{\alpha}$, $^{13}C_{\beta}$, and carbonyl ^{13}C chemical shift data are represented by the square bars. Zero represents the chemical shift of random coil, and −1 and +1 square bars represent the positive and negative deviations of the chemical shifts from random coil values observed in α-helices and β-strands, respectively.

cysteine residues and is only stable for extended periods in the presence of a large excess of reduced DTT. Even under these conditions, the sample degraded over the course of several months, necessitating the recording of spectra only on freshly purified material.

The secondary structure of human glutaredoxin is comprised of five α-helices and four β-strands. The α-helical secondary structure elements were identified by a combination of the characteristic sequential and medium-range NOEs and CSI data with confirmation from the amide proton exchange data.

The first α-helix runs from residue 4 to residue 10. This helix shows strong d_{NN} NOEs for residues 4–10. A pair of medium-range NOEs indicates the N-terminal end of this helix to be residue 4. The paucity of medium-range NOEs observed for this helix and the observation of only a single slowly exchanging amide proton in this region indicate that this is not a very stable helix. Helix 2 extends from residue 24 to residue 36. In contrast to the first helix, strong d_{NN} NOEs and a dense array of medium-range NOEs were observed for this helix. Good agreement with the CSI data is observed and a number of slowly exchanging amide protons were identified in this helix. The third helix extends from residue 53 to residue 64 and again shows a dense array of medium-range NOEs characteristic of helices, good agreement with the CSI results, and a number of slowly exchanging amide protons. The fourth and fifth helices were identified as one long helix from CSI data. However, there is a disruption of the dense network of medium-range NOEs around Gly 93. Thus, two separate helices exist, which extend from residue 83 to residue 92 and from residue 94 to residue 104. As with the second and third helices, a dense array of characteristic medium-range NOEs has been identified that are in good agreement with CSI results and identification of slowly exchanging amide protons.

The β-strands were identified by a combination of strong $d_{\alpha N}$ NOEs, CSI data, identification of slowly exchanging amide protons, and characteristic interstrand NOEs. The first β-strand extends from Val 15 to Ile 19. Strong $d_{\alpha N}$ NOEs and CSI data identify this as a β-strand. In addition, all of these residues exhibit slowed amide proton exchange, indicative of an inner strand in a β-sheet. The second β-strand extends from Leu 43 to Ile 48, with strong $d_{\alpha N}$ NOEs observed throughout and good agreement with the CSI data. Unlike the first β-strand, there are a number of residues that exhibit rapid amide proton exchange indicative of an outer strand in a β-sheet. The last two β-strands are very short, extending from Pro 71 to Ile 75 and from Asp 78 to Ile 80, respectively. Strong $d_{\alpha N}$ NOEs are observed in both β-strands; however, the CSI does not identify these elements as β-strands. The CSI data for all the nuclei of reduced human glutaredoxin are shown in Figure 4. As indicated in Figure 4, residues 71–74 show αH and CO chemical shifts characteristic of β-strands; however, the C_{α} and C_{β} chemical shifts are indicative of coil conformations, thus this strand was not identified in the consensus CSI data. The short β-strand from D78 to I80 shows almost exclusively coil conformation in the CSI analysis. Interestingly, the short strand in the analogous position in *E. coli* Grx1 is highly twisted (Sodano et al., 1991; Bushweller et al., 1994), which may also account for the chemical shift data here. All of the residues involved in these two strands exhibit slowed amide proton exchange with the exception of Cys 79. Thus, β3 appears to be an inner strand in the sheet, whereas β4 is predicted to be an outer strand. The CSI predicts a fifth β-strand extending from Thr 65 to Val 70; however, strong d_{NN} NOEs are observed for a number of these residues, so this has not been identified as a β-strand. In *E. coli* Grx1, this region of the chain does form an extended structure, but it also was not identified as a β-strand.

The four β-strands of human glutaredoxin combine to form a four-stranded β-sheet with the same topology as that observed in *E. coli* Grx1 and in pig liver glutaredoxin (Katti et al., 1995). This topology was established on the basis of characteristic interstrand NH-NH, NH-αH, and αH-αH NOEs identified in the three-dimensional ^{15}N-edited and ^{13}C-edited NOESY spectra. The overall topology of the four-stranded β-sheet identified in human glutaredoxin is depicted in Figure 5.

Structural studies of *E. coli* glutaredoxin-1 (Sodano et al., 1991; Xia et al., 1992; Bushweller et al., 1994), phage T4 glutaredoxin (Eklund et al., 1992; Ingelman et al., 1995), and pig liver thioltransferase (glutaredoxin) (Katti et al., 1995) have shown them to contain a *cis*-proline in the vicinity of the active site; therefore, we

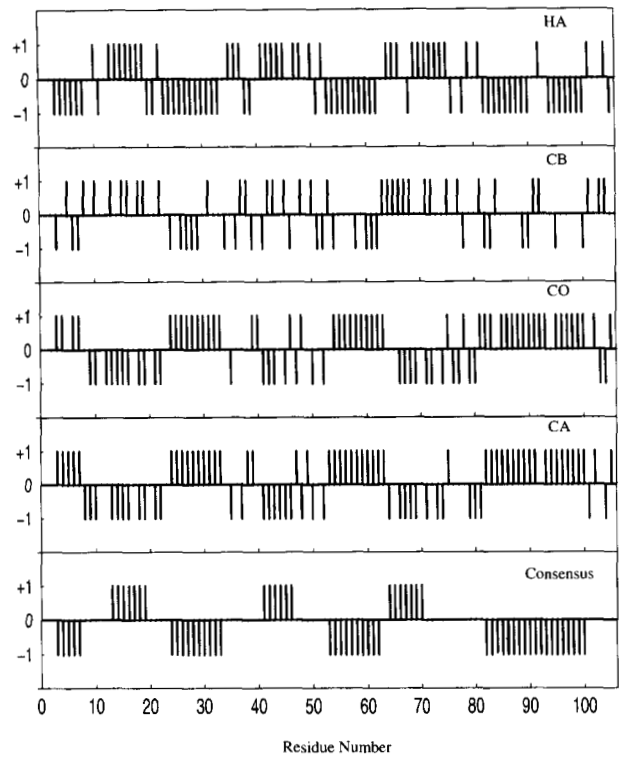

Fig. 4. CSI data derived from H_α, C_α, C_β, CO chemical shifts and the consensus CSI data for reduced human glutaredoxin. The proton chemical shifts are relative to internal 2,2-dimethyl-3-silapentane-5-sulfonic acid (DSS). The ^{15}N and ^{13}C chemical shifts are relative to liquid ammonia and to sodium 2,2-tetradeutero-3-trimethyl-silylpropionate (TSP), respectively (Live et al., 1984; Bax and Subramanian, 1986). Zero refers to the chemical shifts of the random coil structure, whereas +1 and −1 represent the positive and negative deviation of chemical shifts from random coil values.

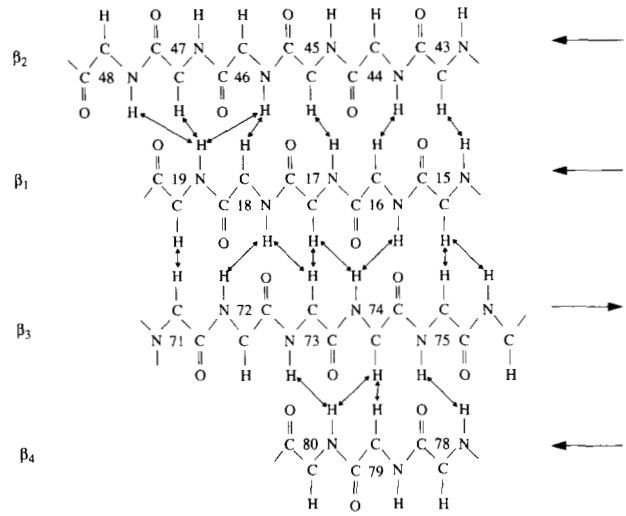

Fig. 5. Schematic arrangement of the β-sheet identified in reduced human glutaredoxin. In the four-stranded sheet, the backbone atoms, the H_α protons, the amide protons, and the carbonyl oxygen atoms are drawn. The sequence locations are indicated near the C_α atoms. Arrows indicate experimental interstrand NOEs between backbone protons observed in the three-dimensional ^{15}N-edited NOESY and/or ^{13}C-edited NOESY spectra.

have examined the ^{13}C-edited NOESY data for the sequential αH-αH and αH-δH NOEs characteristic of *cis* and *trans* prolines, respectively. All the prolines except Pro 71 show strong NOEs from their δH to the αH of the preceding residue, indicating they are *trans*. Pro 71 shows a very strong NOE from its αH to the αH of Val 70, indicating that it is in the *cis* configuration in agreement with the prediction based on the *E. coli* protein and the homology between the two proteins in this region.

The availability of detailed structural information for *E. coli* Grx1 (Sodano et al., 1991; Xia et al., 1992; Bushweller et al., 1994) allows comparisons with human glutaredoxin to be made. The four-stranded β-sheet identified in human glutaredoxin is virtually identical to that observed in *E. coli* Grx1, with a similar number of residues identified in the β-strands and the same topology. The differences between the two structures arise predominantly in the α-helical secondary structure elements. Human glutaredoxin contains additional α-helices at the N and C termini, not found in *E. coli* Grx1, which helps to account for its extended length. The second helix in human glutaredoxin (first in *E. coli* Grx1) is shorter by four residues, or one full turn, than that seen in *E. coli* Grx1. Interestingly, the recent secondary structure determination of *E. coli* Grx3 has also shown this helix to be shortened by one turn relative to that seen in Grx1 (Aslund et al., 1996). The difference in helix 2 in human glutaredoxin is likely to be functionally important because the analogous helix in Grx1 has been suggested to be part of the surface through which glutaredoxin interacts with its protein disulfide substrates (Xia et al., 1992).

The structure of oxidized pig liver thioltransferase (glutaredoxin) has been determined by X-ray crystallography (Katti et al., 1995). As indicated in Figure 1, all the mammalian glutaredoxins show a high degree of similarity in their primary sequences, therefore it is of interest to compare the secondary structural elements of human and pig liver glutaredoxin. Secondary structural elements in the pig liver structure were identified using the program PROCHECK (Laskowski et al., 1993; Rullmann, 1996). This analysis shows both proteins to be comprised of a four-stranded β-sheet and five helices. The helices in the pig liver structure span residues 2–10, 23–34, 53–64, 82–90, and 93–101, whereas the helices identified in human glutaredoxin by NMR span residues 4–10, 24–36, 53–64, 83–92, and 94–104. The four-stranded β-sheet in pig liver glutaredoxin is comprised of residues 14–18, 42–46, 71–74, and 77–80, whereas the corresponding β-sheet residues in human glutaredoxin are 15–19, 43–48, 71–75, and 78–80. The two proteins exhibit virtually identical secondary structural elements. The small differences observed may be attributable to the difficulty in identifying the ends of secondary structural elements solely by NOEs. The last two helices of human glutaredoxin arise from a Gly disruption in what would otherwise be one extended helix. In the pig liver glutaredoxin structure, this Gly results in a significant bend between the two helices. Detailed comparisons between the two structures will have to await the determination of the high-resolution solution structure of human glutaredoxin, which is in progress.

Because there are now NMR resonance assignments available for *E. coli* Grx1 in several forms (Sodano et al., 1991; Xia et al., 1992; Bushweller et al., 1994), *E. coli* Grx3 (Aslund et al., 1996), and human glutaredoxin, comparisons between the three, particularly in the active site region, may provide useful insights. The ^1H chemical shifts for the active site residues of all three proteins in the fully reduced form are given in Table 1. The agreement of the chemical shifts among the three proteins is excellent and indicates

Table 1. *Chemical shifts in ppm of active site residues*

	Human Grx	*E. coli* Grx1	*E. coli* Grx3
NH(C)	C23 7.20	C11 7.26	C11 6.95
αH(C)	4.85	5.07	4.78
αH(P)	P24 4.25	P12 4.29	P12 4.43
NH(Y)	Y25 9.33	Y13 9.14	Y13 9.43
αH(Y)	4.40	3.96	4.37
NH(C)	C26 9.60	C14 9.41	C14 9.79
αH(C)	3.94	4.13	3.94

clearly that the local environment in the active site is quite similar in all three. In all three cases, the NH of the residue preceding the N-terminal Cys of the active site (Gly 10 in *E. coli* Grx1, Thr 10 in *E. coli* Grx3, and Thr 22 in human Grx) has not been observed. No significant broadening of the side-chain ^{1}H or ^{13}C resonances of Thr 22 is observed for human Grx; thus this appears to be a result of extremely rapid NH exchange. In all the known glutaredoxins, the pK_a of the thiol at position 23 in human Grx is very low, ≤4.5 (Gan & Wells, 1987b; Björnberg, 1990; Mieyal et al., 1991); thus the local environment must be highly positively charged to stabilize the thiolate to such an extent. This may offer an explanation for the extremely rapid NH exchange for this position in the glutaredoxins. In the structure of oxidized T4 glutaredoxin, a hydrogen bond was identified from the backbone amide NH of Cys 17 (Cys 26 in human Grx) to the sulfur of Cys 14 (Cys 23 in human Grx) in the active site and this was suggested as one mechanism for stabilization of the thiolate and thus the low pK_a. As seen in Table 1, the amide NH resonance for the second cysteine residue in all three proteins is shifted very far downfield from the random coil value (ca. 8.3 ppm). Additionally, for *E. coli* Grx1, there is a 0.54-ppm downfield shift for this NH upon going from the oxidized to the reduced form (Sodano et al., 1991; Xia et al., 1992). Such large downfield shifts are consistent with hydrogen bonding to a charged group (Bündi & Wüthrich, 1979) and suggest that this NH does play a role in the stabilization of the thiolate in the glutaredoxin family of proteins.

Conclusions

We have completed the sequence-specific NMR resonance assignments of the ^{1}H, ^{13}C, and ^{15}N nuclei of human glutaredoxin in its fully reduced form. The secondary structure of the human protein shows it to be an α/β protein consisting of a four-stranded β-sheet and five α-helices. Comparison with the structure of *E. coli* Grx1 shows that the human protein contains an identical four-stranded β-sheet to that seen in *E. coli* Grx1, but that there are significant differences in the helical secondary structure elements between the two proteins. The secondary structure of human glutaredoxin is very similar to that of pig liver thioltransferase. The completion of the assignments for this protein sets the stage for the determination of its solution structure, which will provide useful insights into the nature of the interaction between human glutaredoxin and its protein disulfide substrates, namely ribonucleotide reductase, and also provide a structural basis for the role of the other cysteine residues in human glutaredoxin as a potential motif for redox regulation of the enzyme as well as perhaps for the TGF-β family of proteins.

Materials and methods

Sample preparation

Human glutaredoxin was expressed and purified from *E. coli* strain BL21(DE2)LysS harboring the plasmid pET-grx according to a modification of the procedure described by Padilla et al. (1995).

A minimal media containing 15 g/L Na_2HPO_4, 2 g/L KH_2PO_4, 0.5 g/L NaCl, 0.473 g/L Na_2SO_4, 1 g/L $(NH_4)_2SO_4$, 4 g/L sugar mix (EMBL, Heidelberg), 1 mg/L thiamine, 1 mg/L biotin, 0.25 g/L Mg_2SO_4, 33 mg/L $CaCl_2$, 100 mg/mL ampicillin, and 20 mg/mL chloramphenicol was used for isotope enrichment of protein samples. ^{15}N and ^{13}C were incorporated into the protein by growing the cells in this media with 1 g/L $^{15}(NH_4)_2SO_4$ and 4 g/L uniformly labeled $^{13}C/^{15}N$ sugar mix (EMBL, Heidelberg) as the sole nitrogen and carbon sources, respectively. Protein concentration was determined by measured OD_{280}.

NMR spectroscopy

The buffer used for NMR studies was 50 mM potassium phosphate, pH 6.0, 0.1 mM EDTA, 5 mM DTT, 0.1% NaN_3, and 5% D_2O.

All NMR measurements were made at 30 °C on a Varian UNITYplus 500 spectrometer equipped with an actively shielded gradient triple resonance probe and pulsed field gradients. In all experiments, no sample spinning was used. Carrier frequencies were typically 4.72 ppm for ^{1}H, 117 ppm for ^{15}N, 45 ppm for aliphatic ^{13}C, 58 ppm for $^{13}C_\alpha$, and 177 ppm for $^{13}C'$.

All the NMR experiments used for assignments and secondary structure determinations are shown in Table 2.

For measurement of the amide-proton exchange rates, 525 μL of fully protonated 0.8 mM protein in 50 mM phosphate buffer at pH 6.0 was lyophilized. Lyophilized protein was dissolved in $^{2}H_2O$ and quickly transferred to the NMR tube at 4 °C. The NMR sample was inserted into the preshimmed spectrometer at 10 °C. After additional shimming, data acquisition started 30 min after the protein was dissolved. A series of two-dimensional [^{15}N, ^{1}H] HSQC spectra were recorded, with each spectrum lasting 2 h. Resonances that were still present in the first HSQC spectrum were deemed slowly exchanging.

Data processing

NMR data were processed using the program PROSA (Güntert et al., 1992). Forward linear prediction was used to extend the time-domain data in all the ^{15}N and ^{13}C dimensions. Zero-filling was applied to all the indirect dimensions. Visualization and analysis of all the spectral data were performed using the program XEASY (Bartels et al., 1995).

Supplementary material in Electronic Appendix

^{1}H, ^{13}C, and ^{15}N assignments for all 105 residues of human glutaredoxin are given in the Electronic Appendix.

Acknowledgments

We are grateful to Dr. C. Alicia Padilla for providing recombinant human glutaredoxin DNA and helpful discussions. We also thank Mr. Wayne Casey for his help in maintaining the NMR spectrometer.

Table 2. *NMR experiments employed for assignments and secondary structure determination for reduced human glutaredoxin*

	Spectra recorded	Dimensions	References
Backbone	2D [^{15}N, ^{1}H]-COSY	128* × 1024*	Otting & Wüthrich, 1988
	DQF-COSY	512* × 1024*	Rance et al., 1983
	TQF-COSY	500* × 1024*	Muller et al., 1986
	Filtered [^{15}N, ^{1}H]-HMQC	128* × 1024*	Kay & Bax, 1989
	3D-^{15}N edited[^{1}H, ^{1}H] NOESY	32* × 128* × 512*	Gronenborn et al., 1989
	3D-^{15}N edited [^{1}H, ^{1}H] TOCSY	32* × 128* × 512*	Gronenborn et al., 1989
	3D CT-HNCA	32* × 48* × 512*	Grzesiek & Bax, 1992
	3D CT-HN(CO)CA	32* × 48* × 512*	Grzesiek & Bax, 1992
	3D HNCACB	32* × 36* × 512*	Muhandiram & Kay, 1994
	3D HN(CA)HA	32* × 64* × 512*	Clubb et al., 1992
	3D HNCO	32* × 64* × 512*	Kay et al., 1994
Side-chain	2D [^{13}C, ^{1}H] CT-HSQC	256* × 1024*	Vuister & Bax, 1992
	3D HCCH-TOCSY (mixing time = 7 ms and 21 ms)	32* × 128* × 512*	Kay et al., 1993
	3D HCCH-COSY	28* × 128* × 512*	Ikura et al., 1991
Aromatic	$(H_\beta)C_\beta(C_\gamma C_\delta)H_\delta$	32* × 512*	Yamazaki et al., 1993
	$(H_\beta)C_\beta(C_\gamma C_\delta C_\epsilon)H_\epsilon$	32* × 32* × 512*	
Secondary structure	^{15}N-edited NOESY-HSQC	32* × 128* × 512*	Zhang et al., 1994
	^{13}C-edited NOESY-HSQC (mixing time = 60 ms)	40* × 124* × 512*	Muhandiram et al., 1993

References

Ahn BY, Moss B. 1992. Glutaredoxin homolog encoded by vaccinia virus is a virion-associated enzyme with thioltransferase and dehydroascorbate reductase activities. *Proc Natl Acad Sci USA 89*:7060–7064.

Aslund F, Nordstrand K, Berndt KD, Nikkola M, Bergman T, Ponstingl H, Jörnvall H, Otting G, Holmgren A. 1996. Glutaredoxin-3 from *Escherichia coli*; amino acid sequence, ^{1}H and ^{15}N NMR assignments and structural analysis. *J Biol Chem 271*:6736–6745.

Bartels C, Xia T, Billeter M, Güntert P, Wüthrich K. 1995. The program XEASY for computer-supported NMR spectral-analysis of biological macromolecules. *J Biomol NMR 6*:1–10.

Bax A, Subramanian S. 1986. Sensitivity-enhanced two-dimensional heteronuclear shift correlation NMR spectroscopy. *J Magn Reson 67*:565–569.

Björnberg O. 1990. Glutaredoxin from *Escherichia coli*; high level expression and characterization of the redox-active center [thesis].

Bündi A, Wüthrich K. 1979. Use of amide ^{1}H-NMR titration shifts for studies of polypeptide conformation. *Biopolymers 18*:299–311.

Bushweller JH, Billeter M, Holmgren A, Wüthrich K. 1994. The NMR solution structure of the mixed disulfide between *E. coli* glutaredoxin (C14S) and glutathione. *J Mol Biol 235*:1585–1597.

Clubb RT, Thanabal V, Wagner G. 1992. A new 3D HN(CA)HA experiment for obtaining fingerprint HN-H_α cross peaks in ^{15}N- and ^{13}C-labeled proteins. *J Biomol NMR 2*:203–210.

Dyson HJ, Gippert GP, Case DA, Holmgren A, Wright PE. 1990. Three-dimensional solution structure of the reduced form of *Escherichia coli* thioredoxin determined by nuclear magnetic resonance spectroscopy. *Biochemistry 29*:4129–4136.

Eklund H, Ingelman M, Söderberg BO, Uhlin T, Nordlund P, Nikkola M, Sonnerstam U, Joelson T, Petratos K. 1992. Structure of oxidized bacteriophage T4 glutaredoxin (thioredoxin). *J Mol Biol 228*:596–618.

Forman-Kay JD, Clore GM, Wingfield PT, Gronenborn AM. 1991. High-resolution three-dimensional structure of reduced recombinant thioredoxin in solution. *Biochemistry 30*:2685–2698.

Gan ZR, Polokoff MA, Jacobs JW, Sordana MK. 1990. Complete amino acid sequence of yeast thioltransferase (glutaredoxin). *Biochem Biophys Res Commun 168*:944–951.

Gan ZR, Wells WW. 1987a. The primary structure of pig liver thioltransferase. *J Biol Chem 262*:6699–6703.

Gan ZR, Wells WW. 1987b. Identification and reactivity of the catalytic site of pig liver thioltransferase. *J Biol Chem 262*:6704–6797.

Gravina SA, Mieyal JJ. 1993. Thioltransferase is a specific glutathionyl mixed disulfide oxidoreductase. *Biochemistry 32*:3368–3376.

Gronenborn AM, Bax A, Wingfield PT, Clore GM. 1989. A powerful method of sequential proton resonance assignment in proteins using relayed ^{15}N-^{1}H multiple quantum coherence spectroscopy. *FEBS Lett 243*:93–98.

Grzesiek S, Bax A. 1992. Improved 3D triple-resonance NMR techniques applied to a 31 kDa protein. *J Magn Reson 96*:432–440.

Guigó R, Smith TF. 1991. A common pattern between the TGF-β family and glutaredoxin. *Biochem J 280*:833–834.

Güntert P, Dötsch V, Wider G, Wüthrich K. 1992. Processing of multi-dimensional NMR data with the new software PROSA. *J Biomol NMR 2*:619–629.

Holmgren A. 1976. Hydrogen donor system for *Escherichia coli* ribonucleoside-diphosphate reductase dependent upon glutathione. *Proc Natl Acad Sci USA 73*:2275–2279.

Holmgren A. 1979a. Glutathione-dependent synthesis of deoxyribonucleotides. Purification and characterization of glutaredoxin from *Escherichia coli*. *J Biol Chem 254*:3664–3671.

Holmgren A. 1979b. Reduction of disulfides by thioredoxin. Exceptional reactivity of insulin and suggested functions of thioredoxin in mechanism of hormone action. *J Biol Chem 254*:9113–9119.

Holmgren A. 1985. Thioredoxin. *Annu Rev Biochem 54*:237–271.

Holmgren A. 1989. Thioredoxin and glutaredoxin systems. *J Biol Chem 264*: 13963–13966.

Höög JO, Jörnvall H, Holmgren A, Carlquist M, Persson M. 1983. The primary structure of *Escherichia coli* glutaredoxin. *Eur J Biochem 136*:223–232.

Hopper S, Johnson RS, Biemann K. 1989. Glutaredoxin from rabbit bone marrow. Purification, characterization and amino acid sequence determination by tandem mass spectrometry. *J Biol Chem 264*:20438–20447.

Ikura M, Kay LE, Bax A. 1991. Improved three-dimensional ^{1}H-^{13}C-^{1}H correlation spectroscopy of a ^{13}C-labeled protein using constant-time evolution. *J Biomol NMR 1*:299–304.

Ingelman M, Nordlund P, Eklund H. 1995. The structure of a reduced mutant T4 glutaredoxin. *FEBS Lett 370*:209–211.

Jeng MF, Campbell AP, Begley T, Holmgren A, Case DA, Wright PE, Dyson HJ. 1994. High-resolution structures of oxidized and reduced *Escherichia coli* thioredoxin. *Structure 2*:853–868.

Johnson GP, Goebel SJ, Perkus ME, Davis SW, Winslow JP, Paoletti E. 1991. Vaccinia virus encodes a protein with similarity to glutaredoxins. *Virology 181*:378–381.

Katti SK, LeMaster DM, Eklund H. 1990. Crystal structure of thioredoxin from *Escherichia coli* at 1.68 Å resolution. *J Mol Biol 212*:167–184.

Katti SK, Robbins AH, Yang Y, Wells WW. 1995. Crystal structure of thioltransferase at 2.2 Å resolution. *Protein Sci 4*:1998–2005.

Kay LE, Bax A. 1989. Separation of NH and NH_2 resonances in ^{1}H-detected heteronuclear multiple-quantum correlation spectra. *J Magn Reson 84*:598–603.

Kay LE, Xu GY, Singer AU, Muhandiram DR, Forman-Kay JD. 1993. A gradient-enhanced HCCH-TOCSY experiment for recording side-chain ^{1}H and ^{13}C correlations in H_2O samples of proteins. *J Magn Reson B 101*:333–337.

Kay LE, Xu GY, Yamazaki T. 1994. Enhanced-sensitivity triple resonance spectroscopy with minimal H_2O saturation. *J Magn Reson A 109*:129–133.

Klintrot IM, Höög JO, Jörnvall H, Holmgren A, Luthman M. 1984. The primary structure of calf thymus glutaredoxin. Homology with the corresponding *Escherichia coli* protein but elongation at both ends with an additional half-cysteine/cysteine pair. *Eur J Biochem 144*:417–423.

Laskowski RA, MacArthur MW, Moss DS, Thornton JM. 1993. PROCHECK: A program to check the stereochemical quality of protein structure. *J Appl Crystallogr 26*:283–291.

Live DH, Davis DG, Agosta WC, Cowburn D. 1984. Long range hydrogen bond mediated effects in peptides: ^{15}N NMR study of Gramicidin S in water and organic solvents. *J Am Chem Soc 106*:1939–1941.

Luthman M, Eriksson S, Holmgren A, Thelander L. 1979. Glutathione-dependent hydrogen donor system for calf thymus ribonucleoside diphosphate reductase. *Proc Natl Acad Sci USA 76*:2158–2162.

Luthman M, Holmgren A. 1982. Glutaredoxin from calf thymus. I. Purification to homogeneity. *J Biol Chem 257*:6686–6690.

Mieyal JJ, Starke DW, Gravina SA, Hocevar BA. 1991. Thioltransferase in human red blood cells: Kinetics and equilibrium. *Biochemistry 30*:8883–8891.

Minakuchi K, Yabushita T, Masumura T, Ichihara K, Tanaka K. 1994. Cloning and sequence analysis of a cDNA encoding rice glutaredoxin. *FEBS Lett 337*:157–160.

Muhandiram DR, Farrow NA, Xu GY, Smallcombe SH, Kay LE. 1993. A gradient ^{13}C NOESY-HSQC experiment for recording NOESY spectra of ^{13}C-labeled proteins dissolved in H_2O. *J Magn Reson B 102*:317–321.

Muhandiram DR, Kay LE. 1994. Gradient enhanced triple-resonance three-dimensional NMR experiments with improved sensitivity. *J Magn Reson B 103*:203–216.

Muller N, Ernst RR, Wüthrich K. 1986. Multi-quantum-filtered two-dimensional correlated NMR spectroscopy of proteins. *J Am Chem Soc 108*:6482–6492.

Otting G, Wüthrich K. 1988. Efficient purging scheme for proton-detected heteronuclear two-dimensional NMR. *J Magn Reson 76*:569–574.

Padilla CA, Martinez-Galisteo E, Bárcena JA, Spyrou G, Holmgren A. 1995. Purification from placenta, amino acid sequence, structure comparisons and cDNA cloning of human glutaredoxin. *Eur J Biochem 227*:27–34.

Padilla CA, Spyrou G, Holmgren A. 1996. High-level expression of fully active human glutaredoxin (thioltransferase) in *E. coli* and characterization of Cys 7 to Ser mutant protein. *FEBS Lett 378*:69–73

Papayannopoulos IA, Gan ZR, Wells WW, Biemann K. 1989. A revised sequence of calf thymus glutaredoxin. *Biochem Biophys Res Commun 159*: 1448–1454.

Qin J, Clore GM, Gronenborn AM. 1994. The high-resolution three-dimensional solution structures of the oxidized and reduced states of human thioredoxin. *Structure 2*:503–522.

Rance M, Snilrensen O, Bodenhausen G, Wagner G, Ernst RR, Wüthrich K. 1983. Improved spectral resolution in COSY ^{1}H NMR spectra of proteins via double quantum filtering. *Biochem Biophys Res Commun 117*:479–485.

Rullmann JAC. 1996. AQUA, computer program, Department of NMR Spectroscopy, Bijvoet Center for Biomolecular Research, Utrecht University, The Netherlands.

Sodano P, Xia T, Bushweller JH, Björnberg O, Holmgren A, Billeter M, Wüthrich K. 1991. Sequence-specific ^{1}H n.m.r. assignments and determination of the three-dimensional structure of reduced *Escherichia coli* glutaredoxin. *J Mol Biol 221*:1311–1324.

Spera S, Bax A. 1991. Empirical correlation between protein backbone conformation and C_α and C_β ^{13}C nuclear magnetic resonance chemical shifts. *J Am Chem Soc 113*:5490–5492.

Vuister GW, Bax A. 1992. Resolution enhancement and spectral editing of uniformly ^{13}C-enriched proteins by homonuclear broadband ^{13}C decoupling. *J Magn Reson 98*:428–435.

Wells WW, Xu DP, Yang YF, Rocque PA. 1990. Mammalian thioltransferase (glutaredoxin) and protein disulfide isomerase have dehydroascorbate reductase activity. *J Biol Chem 265*:15361–15364.

Wishart DS, Sykes BD. 1994. The ^{13}C chemical shift index: A simple method for the identification of protein secondary structure using ^{13}C chemical shift data. *J Biomol NMR 4*:171–180.

Wittekind M, Mueller L. 1993. HNCACB, a high-sensitivity 3D NMR experiment to correlate amide-proton and nitrogen resonances with the alpha- and beta-carbon resonances in proteins. *J Magn Reson B 101*:201–205.

Wüthrich K. 1986. *NMR of protein and nucleic acids*. New York: John Wiley.

Xia T, Bushweller JH, Sodano P, Billeter M, Björnberg O, Holmgren A, Wüthrich K. 1992. NMR structure of oxidized *Escherichia coli* glutaredoxin: Comparison with reduced *E. coli* glutaredoxin and functionally related proteins. *Protein Sci 1*:310–321.

Yamazaki T, Forman-Kay JD, Kay LE. 1993. Two-dimensional NMR experiments for correlating $^{13}C_\beta$ and $^{1}H_{\delta/\epsilon}$ chemical shifts of aromatic residues in ^{13}C-labeled proteins via scalar couplings. *J Am Chem Soc 115*:11054–11055.

Zhang O, Kay LE, Olivier JP, Forman-Kay JD. 1994. Backbone ^{1}H and ^{15}N resonance assignments of the N-terminal SH3 domain of drk in folded and unfolded states using enhanced sensitivity pulsed field gradient NMR techniques. *J Biomol NMR 4*:845–858.

Ziegler DM. 1985. Role of reversible oxidation–reduction of enzyme thiols-disulfides in metabolic regulation. *Annu Rev Biochem 54*:305–329.